CHAPTER 1

Review of existing density determinations

1.1 Introduction

Modern developments in geophysics, geology and engineering have resulted in increasingly sophisticated techniques of analysis of problems in soil mechanics. The reasons for this are threefold:

- Better and more sophisticated technology are more readily available.
- The need to determine parameters more accurately.
- The need to decrease the cost of development projects.

These improved methods have also highlighted the problems inherent to conventional sampling and laboratory testing procedures. Frequently, these testing procedures cannot supply suitable accurate parameters for either sophisticated techniques of analysis (such as finite element analysis) or even for modern design calculations.

Various authors have shown that the action of 'sampling' causes significant disturbance due to mechanical deformation and to the inevitable difference in stress history between a sampled element of subsurface and a similar element in the field (Davis and Poulos,1966). This confirms the need to sample physical properties in-situ (for example density and small movement elasticity modulus), in particular for the construction and engineering industry.

Although tests like the Dynamic Cone Penetrometer Test and the consolidation test can give an indication of density variations in the subsurface, accurate in-situ density determinations could up to now, only be determined down to a shallow depth by using the neutron based Troxler equipment. Variations in the moisture content can however influence these determinations. If accurate density and other subsurface

parameters are needed from greater depths, an undisturbed sample is needed. Physical properties derived from field geophysical techniques tend to be much larger than those obtained from conventional laboratory testing, for example stiffnesses derived from field seismics (Clayton C.R.I. and Heyman G., 2001). A laser interferometry system was developed to evaluate the sensitivity and accuracy of displacement transducers (Heyman G., Clayton C.R.I., and Reed G.T., 1997) in order to investigate the extent of the linear-elastic range of geomaterials in triaxial stress space.

This argument has led in the past to the belief that geophysical measurements are useful in design problems associated with large events like earthquakes where large movements occur, but could not be used in engineering calculations of small ground movements around foundations and structures. This now raises the question: Is it worth while to develop and apply any geophysical techniques for engineering applications?

It was argued (Auld, 1977) that seismic methods are dynamic, giving negligible time for plastic or creep strains to occur and that the strains that it induces are very small. It was only recently acknowledged that stresses and strains around tunnels are actually very small and allow geophysical techniques the capability to yield these parameters (Jardin et. al, 1986).

It has been shown that the results of the very-small-strain stiffness measured in the laboratory by making use of a Fabry-Perot laser interferometer under high pressure (Clayton C.R.I. and Heyman G., 2001) were comparable with geophysical data from the same sites where the samples were taken. The movements during the seismic experiments were measured using displacement transducers.

This proves that the use of geophysical techniques is suitable in deriving in-situ engineering parameters and that the developments of such geophysical techniques are necessary and advisable.

1.2 Previous Work

1.2.1 Geophysics Related work

In order to emphasize the importance of accurate in-situ measurements on all the physical properties (including densities) vital to engineers, this section will concentrate on important issues from existing literature. The Seismic Refraction method can be used to determine the densities of the subsurface (Griffiths and King, 1969, Darracott, 1976). The densities are obtained indirectly by measuring the velocities of the P-waves and S-waves.

For a P-wave or pressure wave the particle movement is in the same direction as the wave propagation (longitudinal wave). In the case of a S-wave or shear wave the particle movement is perpendicular to the wave propagation (transverse wave). The basic equations describing these velocities are:

$$V_p = \sqrt{\frac{k + \frac{4}{3}G}{\rho}} \qquad\qquad 1.$$

And

$$V_s = \sqrt{\frac{G}{\rho}} \qquad\qquad 2.$$

Where **k** is the elastic (Bulk) or incompressibility modulus, G is the shear or rigidity modulus and ρ is the density.

In a solid with a larger density, the elastic modulus (k) and the shear modulus (G) are larger because it is harder to compress and it is thus more difficult to deform the medium, resulting in larger velocities. It can thus be shown from the above equations, that larger densities are associated with higher velocities. By using the seismic refraction method, the density is measured in-situ. The density value is

however only an indication of the real value due to the large sampling volume, which is directly proportional to the size of the seismic spread (6,12,24 channel and geophone spacing).

Engineers routinely use the ratio of V_p/V_s to get an indication of the density and "hardness" of the subsurface, and generally the following hold true (Darracott, 1976):

- High V_p and a V_p/V_s ratio of approximately $\sqrt{3}$ indicates unweathered bedrock.
- Low V_p and a V_p/V_s ratio of approximately $\sqrt{3}$ indicates sandy or gravel fill.
- Low V_p and a high V_p/V_s ratio indicate clayey material, usually above the water table.
- V_p velocity about 1500 m/s, high V_p/V_s ratio may indicate soft clay material, below the water table.

It is impossible to distinguish between minor layers inside the weathered layer if the velocity contrasts are small. For most rocks there is an empirical relationship between the V_p and the rock quality, namely the higher the velocity the better the rock quality (Brown and Robertshaw, 1953). They determined the empirical relationship between Young's modulus (E) and V_p:

$$E = 111.15V_p^{2.34} \qquad\qquad 3.$$

Where the unit for E is in Pa.

Poisson's ratios can be obtained from seismic velocities (Brown and Robertshaw, 1953). Poisson's ratio is the ratio of transverse contraction strain to longitudinal extension strain in the direction of the stretching force. Tensile deformation is considered positive and compressive deformation is considered negative. The definition of Poisson's ratio contains a minus sign so that the majority of materials have a positive ratio.

$$v = \frac{-\varepsilon_{trans}}{\varepsilon_{longitudinal}} \qquad\qquad 4.$$

Where ε and v are the symbols for deformation and Poisson's ratio. This relationship can be used to obtain:

$$\frac{V_p}{V_s} = \frac{1-v}{\frac{1}{2}-v} \qquad\qquad 5.$$

If the subsurface is compacted, it is found that the elastic modulus k and G increase more rapidly than does the density, which makes the determination of the density difficult (Griffiths and King, 1969). An empirical relationship obtained from experimental results between velocity and density is shown in Figure 1.1,
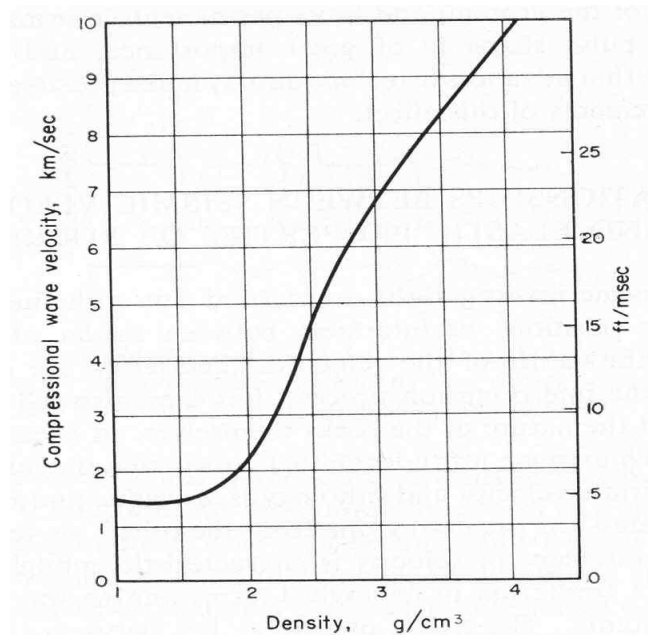

Figure 1.1: Relationship between P-wave velocity and density (after Griffiths and King, 1969)

Data from a particular rock type may fit the form of the graph well, but other variables (mineral composition, cementation, degree of fissuring) should be taken

into account if the velocity and hence density of the material is estimated. This means that if, on the contrary, the velocity has been measured, and an estimate of these other variables is needed then the velocity is to be used to make an accurate estimate of density (Griffiths and King, 1969).

It is difficult to assign a specific velocity and a density to a rock type, but it is possible to quote a range of velocities which would cover a certain lithology. Table 1 is an example:

Lithology	P-wave velocity (km/s)	Density (g/cm^3)
Clastic rocks, unconsolidated	0.3-1.8	1.5-2.2
Clastic rocks, consolidated and cemented	1.5-3.7	2.0-2.6
Clastic rocks in orogenic belts	3.1-6.2	2.5-2.8
Metamorphic rocks	4.6-6.2	2.7-3.0
Limestone	3.1-6.2	2.4-2.7
Igneous rocks	4.6-4.2	2.4-3.0

Table1: P-wave velocities for certain rock types (after Griffith and King, 1969).

Table 1 shows the general trend of increasing velocity with increasing density (i. e. decreasing porosity). It also shows the extend to which rock types can be separated on the basis of seismic velocity. The large areas of overlap indicate the insensitivity of the seismic velocity to small variations in density.

Materials of exceptionally low velocity are usually encountered near the surface (weathered layer) and are of considerable importance to the civil engineer. Properties such as its elasticity (especially the small movement elasticity modulus), plasticity, strength and density are the most important. Young's modulus can only be determined if the velocity, density and Poisson's ratio are known.

The seismic cone test (Heymann, 2003) is used to measure the in situ S and P waves of the soil. The largest advantage of this test is that it allows for the measurement of the void ratio on undisturbed material at in situ stress conditions.

Heymann (2003) used the seismic cone test on a gold tailings dam and compared it with an undisturbed sample from the day wall (outside wall) of the same dam, indicating that the void ratio of the day wall is smaller. According to Heymann (2003) the small strain stiffness and Poisson's ratio can also be calculated from the velocity measurements where small movements occur.

Shear waves provide a direct way of determining the dynamic shear modulus of the ground independent of Poisson's ratio (Abbiss, 1981). In this study two shear wave methods have been applied to determine in situ properties as a function of depth on three clay sites. The first method was shear wave refraction and the second measured the velocity of Rayleigh waves generated by vibrators. In addition pressure wave velocities were measured enabling the dynamic Poisson's ratio to be calculated.

Shear wave methods have the advantage that the shear modulus is directly related to the shear wave velocity (Equation 2, Abbiss, 1981). This is not necessarily the case for the p-wave velocity where the modulus may depend to a large extent on Poisson's ratio.

The modulus of chalk at Munford was compared from a seismic survey and a large tank test (Abbiss, 1979). A steel tank of 18.3m in diameter and approximately 20m high was filled with water to produce a pressure of 179kNm^{-2}. Displacements under the tank were measured in vertical shafts, by means of very accurate displacement transducers. In this way strains were measured at various levels down to 16.3m below the tank, nearly to the water table.

It was found that the dynamic Young's moduli calculated from a seismic refraction survey of the chalk are proportional to the moduli determined from the full scale tank loading test. It corresponds with the finite element analyses of the full scale tank loading test. The moduli showed a linear increase with depth.

The main problem of a shear wave refraction survey is to identify the s-wave arrivals between the p-waves. The best way to remedy the situation is to use a source that is rich in s-waves in the direction of the survey (Abbiss, 1981). The signal to noise ratio can also be improved by stacking the signal. By reversing the connections of the S-wave geophone so that it is out of sequence with the polarity reversals of the source will assist in the stacking of S-wave but will zero the p-wave (Abbiss, 1981).

The density and thickness of the overburden (Depth to bedrock) can also be determined by the gravity method. Techniques and algorithms calculating the depth to basement (Thanassoulas, C. and Tsokas G.N., 1985) of which one was developed by Tsuboi (1983) exist. The smallest thickness (for a single layer) 500m was achieved by Thanassoulas,C. and Tsokas G.N. This indicates that the method is not sensitive enough to distinguish between very thin layers inside a weathered layered profile.

1.2.2 Engineering Geology Related Work

A large variety of field and laboratory tests have been developed and used, of which the "density-in-place" tests are applicable to this study. This test measures the in-place density in a foundation, a borrow area, or a compacted embankment by excavating holes. This is done by weighing the material that is excavated and the volume of the hole is determined by filling it with calibrated sand (Design of small dams, 1965). To obtain a dry density of the sample a water content determination of the excavated material is performed.

Air-dry uniform sand passing through the no. 16 sieve and retained by the no. 30 sieve has been found to be satisfactory. Clean blow sand or dune sand is the most suitable (Design of small dams, 1965). When large test holes are used in gravel soils, coarse sand having rounded particles is recommended. It should pass through the no. 4 sieve but should be retained by the no. 8 sieve. The sand is calibrated by pouring it into a container of known volume of approximately the size

and shape of the type of excavation to be used, weighing it and calculating its unit weight.

At the test location, all loose soil is removed from the area and a work platform is used to support the edges of the excavation (Figure 1.2). This protects the area that is being measured from the weight of the operator, which may deform and change the dimensions of the hole (Design of small dams, 1965). Care must thus be taken not to stand too close to the hole. Although this method gives a good indication of the density, it is not as accurate as an in-situ measurement.

Figure 1.2: Determining density by replacement with sand of known density (After Design of small dams, 1965).

It is sometimes necessary to obtain densities for deeper foundations, which usually penetrate different layers of the subsurface. The following simple method has been used successfully to obtain in-place density in stages of depth in foundations and borrow areas (Design of small dams, 1965):

A platform and auger are used. The platform is set up in such a way that the operator is 1m away from the hole, to prevent damage and compression of the soil around the hole. The auger is used to drill the hole and the soil is saved. The process is repeated until the second layer is reached. The depth of the hole is measured up to the first interface and the removed soil is weighed. The diameter of the hole is known (auger diameter) and the volume can be calculated. These parameters combined with the weight of the soil, enable the calculation of the density of the removed soil. This process is repeated for every layer encountered.

The density or specific gravity of undisturbed samples can also be measured in the laboratory. The no. 4 fraction of the soil is commonly tested by the flask method (Design of small dams, 1965). A 500ml long-necked flask is calibrated for volume at several temperatures. One hundred grams of oven dried soil is washed into the flask with distilled water. A vacuum is applied to the mixture to get rid of all air and the temperature of the mixture is recorded. The weight of the flask with the mixture is then measured. The volume of the 100g soil is calculated and the specific gravity is then computed.

To determine the specific gravity of gravel and cobbles, the material remains immersed in water for 24 hours and is then blotted with a towel. This is the surface-dry condition. It is then weighed and its water displacement is measured.

CHAPTER 2

Theoretical study

2.1 Introduction

In order to obtain the density of the subsurface, without disturbance or damage, it is essential that we must be able to obtain the mass (M_0) and the volume (V_0) of the sample area (Figure 2.1). The challenge lies herein to be able to obtain M_0 and V_0 from indirect sources of measurement, since the direct approaches like drilling is deemed undesirable in some cases.

The method that is proposed tries to measure the mass and the volume of the sample to be investigated through the use of seismic waves, a bearing plate on the surface, a three component geophone and weights to be added to the bearing plate.
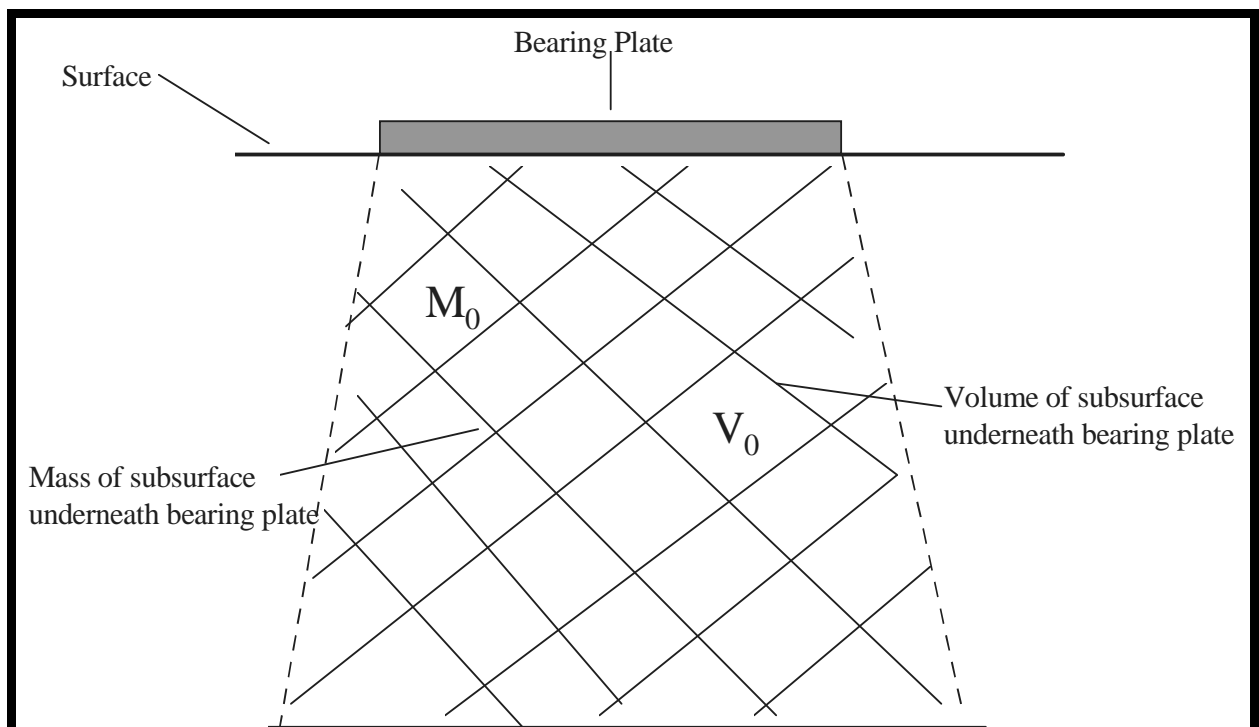
Figure 2.1: Schematic representation of the problem.

In order to try and derive a mathematical model, we make the assumption that we can represent the system by using a very simple model; a mass on a spring that is equal to the mass of the subsurface underneath the bearing plate. The other end of the spring is tied to an edifice (Figure 2.2).
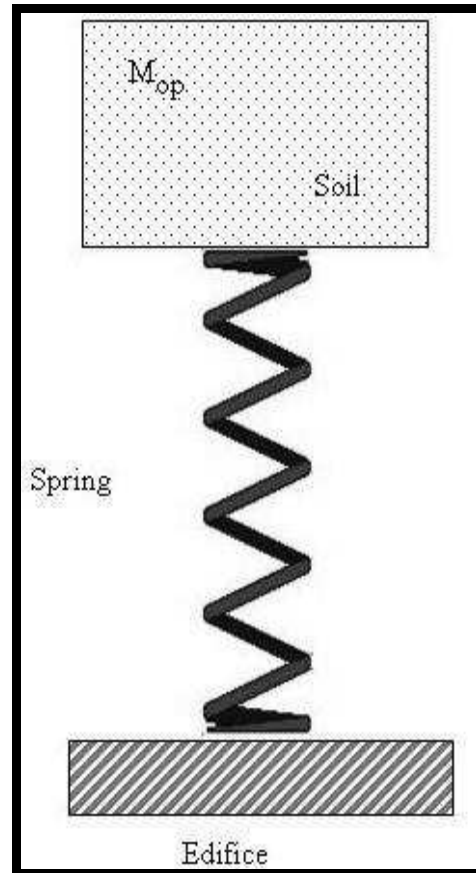

Figure 2.2: Representation of the problem by using a weight on a spring.

2.2 P-wave model

2.2.1 Determination of the mass M_{0p}

From the above assumption we can write the following relation from Hooke's law:

$$F_p = -k_p x_p \qquad\qquad 1$$

Where k_p is the spring constant and x_p is the displacement.

From Newton II:

$$M_{0p}\ddot{x}_p + k_p x_p = 0 \qquad\qquad 2$$

We have further that $k_p = \omega_{0p}^2 M_{0p}$ and that the wave function for displacement is

$$x_p = x_{0p}\sin(\omega_{0p}t + \phi) \qquad\qquad 3$$

To obtain the mass M_{0p} we have to plot the frequency of the vibration versus the increased mass ($M_{0p}+\Delta m$). From equation 2 we have:

$$\ddot{x}_p + \frac{k_p}{M_{0p}}x_p = 0 \qquad\qquad 4$$

And

$$\omega_{0p}^2 = \frac{k_p}{M_{0p}} \qquad\qquad 5$$

Thus

$$k_p = \omega_{p0}^2 M_{0p} \qquad\qquad 6$$

If we add a mass Δm to the mass M_{0p} and k_p stays the same, the angular frequency changes to ω_{1p}^2. Equation 6 then changes to:

$$k_p = \omega_{1p}^2(M_{0p} + \Delta m) \qquad\qquad 7$$

And because:

$$\frac{1}{\omega_{0p}^2} = \frac{1}{k_p}M_{0p} \qquad\qquad 8$$

it implies that

$$\frac{1}{\omega_{1p}^2} = \frac{1}{k_p}(M_{0p} + \Delta m) \qquad\qquad 9$$

13

Equation 9 is a straight line and we also have two unknowns, k_p and M_{0p}. If we rewrite equation 9 a bit we obtain:

$$\frac{1}{\omega_{1p}^2} = \frac{M_{0p}}{k_p} + \frac{\Delta m}{k_p} \qquad\qquad 10$$

Since M_{0p}/k_p is an unknown, it is also a constant, say y_p.

$$\frac{1}{\omega_{1p}^2} = y_p + \frac{\Delta m}{k_p} \qquad\qquad 11$$

or

$$\frac{1}{\omega_{1p}^2} = \frac{1}{k_p}\Delta m + y_p \qquad\qquad 12$$

If we now plot Δm against $1/\omega_{1p}^2$, the slope of the line will be $1/k_p$. M_{0p} can be obtained from y_p or by the extension of the line. Where the line intersects with the Δm axis, the absolute value of M_{0p} can be read off. These values are accurate since the line is straight (Figure.2.3).
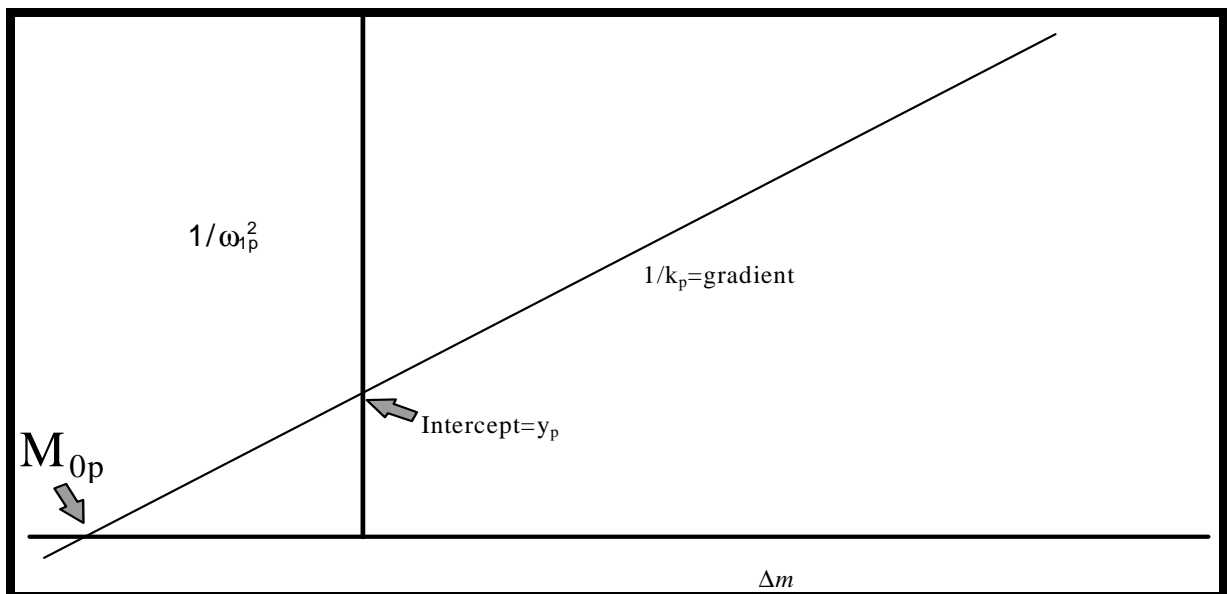
Figure 2.3: Determination of the excited mass.

2.2.2 Determination of the volume V_{0p}.

If we assume that we are going to use a square base plate with side L, and that the diffusion angle from the plate is α, then the resulting area underneath the plate (Figure. 2.4) is the following:
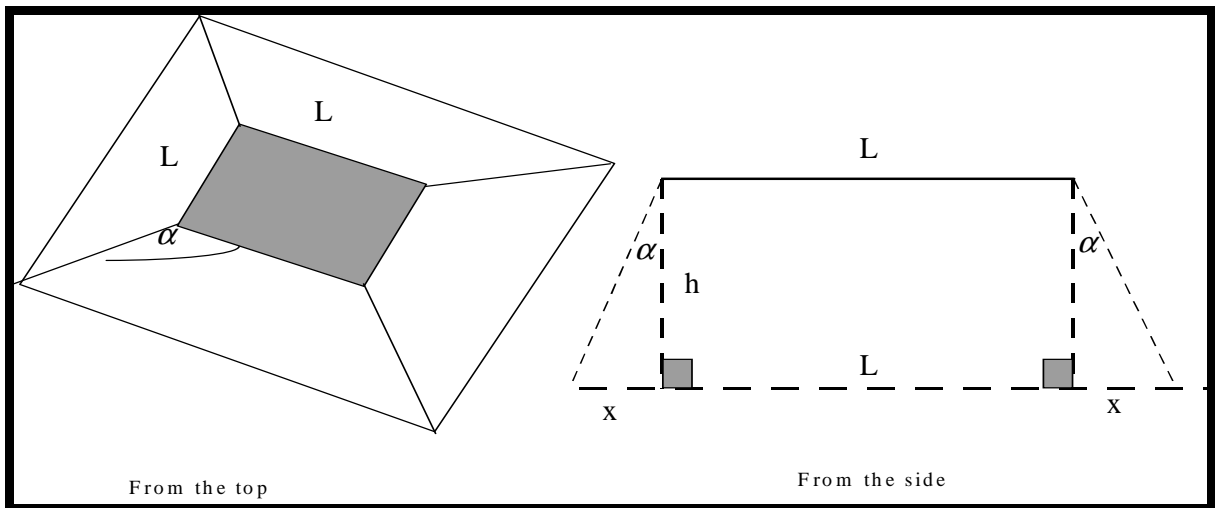

Figure 2.4: Influence of the excited wave underneath the base plate.

The new length is L +2x and since tanα=x/h the new area is:

$$A = (L + 2h_p \tan \alpha)^2 \qquad\qquad 13$$

The volume of the vibrating column $V_{0p} = A \times h_p$. The height of the vibrating volume is unknown. The objective is to express the height of the volume in terms of elements that we can measure, like the wavelength or the velocity of seismic waves.

During the excitation of the ground mass, the movement experiences attenuation. The differential equation that expresses the system is at follows:

$$F_p + b_p v_p = -k_p x_p \qquad\qquad 14$$

15

Where b_p is the attenuation coefficient and v_p is the velocity of the medium.

If we assume that the attenuation factor is dependant on the velocity of the ground movement and that x_p is the differential movement of a differential volume under the plate, then:

$$m_{0p} \frac{d^2 x_p}{dt^2} + b_p \frac{dx_p}{dt} + k_p x_p = 0 \qquad\qquad 15$$

$$\frac{d^2 x_p}{dt^2} + \frac{b_p}{m_{0p}} \frac{dx_p}{dt} + \frac{k_p}{m_{0p}} x_p = 0 \qquad\qquad 16$$

and

$$\frac{d^2 x_p}{dt^2} + \frac{b_p}{m_{0p}\omega_{0p}} \omega_{0p} \frac{dx_p}{dt} + \omega_{0p}^2 x_p = 0 \qquad\qquad 17$$

$$\frac{d^2 x_p}{dt^2} + 2\varepsilon_p \omega_{0p} \frac{dx_p}{dt} + \omega_{0p}^2 x_p = 0 \qquad\qquad 18$$

Where

$$\varepsilon_p = \frac{1}{2} \frac{b_p}{m_{0p}\omega_{0p}} \qquad\qquad 19$$

If we assume that the damping is not much, a solution to this differential equation is:

$$A(\varepsilon)_p = A_{0p} e^{-\varepsilon \omega_{0p} t} \qquad\qquad 20$$

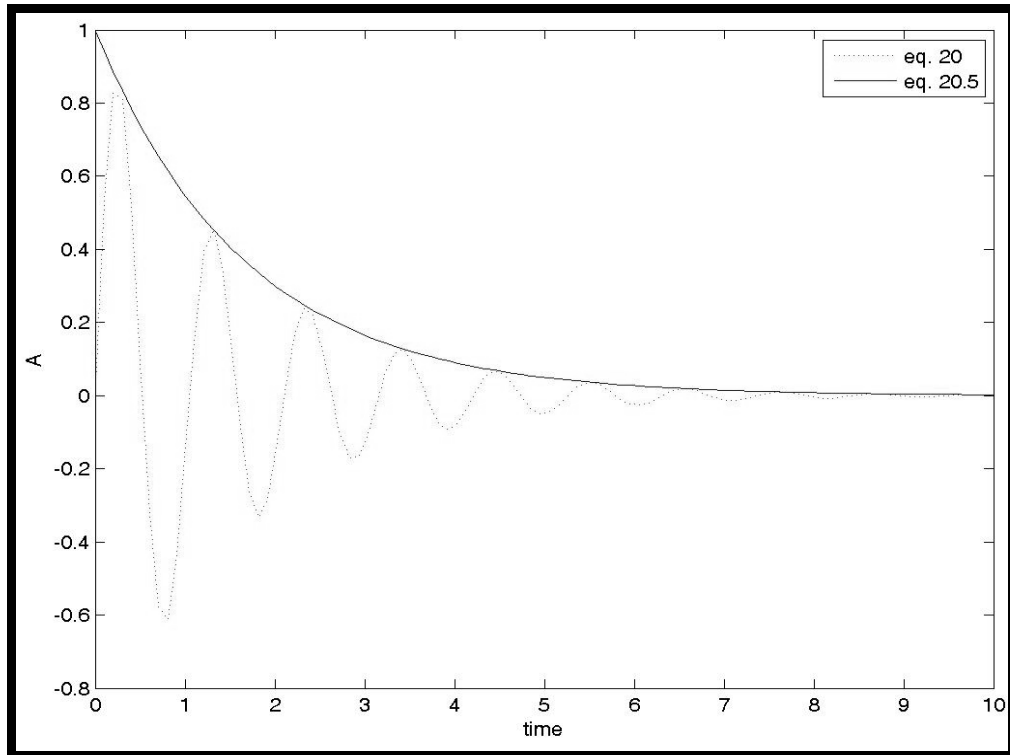This is a harmonic oscillation that decays exponentially with time (Figure 2.5):

Figure 2.5: An example of a Harmonic oscillator that decays exponentially with time.

We can express ε_p in terms of the quality factor Q_p:

$$\varepsilon_p = \frac{1}{2Q_p} \qquad\qquad 21$$

Thus equation 20 changes to:

$$A(\varepsilon)_p = A_{0p}e^{-\omega_{0p}t/2Q_p} \qquad\qquad 22$$

Where Q_p (quality factor) is defined in terms of the fractional loss of energy per cycle of oscillation. In other words:

$$\frac{1}{Q_p} = \frac{-\Delta E_p}{2\pi E_p} \qquad\qquad 23$$

The quality factor can also be expressed in terms of the logarithmic decrement:

$$Q_p = \frac{\pi}{\delta_p}$$

24

If we now substitute equation 24 and the fact that $t = x/v$ and $\omega = 2\pi f$ into equation 22 we get:

$$A(\varepsilon)_p = A_{0p} e^{-(\frac{f_p \pi}{Q_p V_p}) x_p}$$

25

This transforms to

$$A(\varepsilon)_p = A_{0p} e^{-\frac{\psi_p x_p}{\lambda_p}}$$

26

where $f_p/V_p = 1/\lambda_p$ and $\pi/Q_p = \psi_p$. Equation 26 expresses the decrease in amplitude of a wave due to attenuation as a function of distance travelled. ψ_p is an attenuation constant that is frequency dependant. High frequency waves will attenuate more quickly. If we now want to express the decrease in amplitude as a function of depth h_p, we get

$$A(\varepsilon)_p = A_{0p} e^{-\frac{\psi_p h_p}{\lambda_p}}$$

27

The depths that would be investigated will be quite small, and in the order of 3-10m. We can thus assume that the velocity at a depth h_p of the seismic wave is V_p. If we assume that there is no frequency dispersion at these shallow depths ($\omega_p = \omega_{0p}$), and ω_{0p} is on the ground at ($h_p = 0$), we can express the volume as:

$$V_p = A_{0p} \omega_{0p} e^{-\frac{\psi_p h_p}{\lambda_p}}$$

28

The kinetic energy of the column will be equal to the energy of the source. If we now attempt to calculate the kinetic energy of the vibrating column, we get:

$$E_{kp} = \frac{1}{2} m_{0p} v_p{}^2 \qquad\qquad 29$$

If we now examine the kinetic energy of a small volume at a depth h_p, and that $m_p = \rho_p * V_p$ and that Volume (V_p) = $A_p * h_p$ we get

$$dE_{kp} = \frac{1}{2} \rho_p A V_p^2 dh_p \qquad\qquad 30$$

And if we substitute equations 13 and 29 into equation 30,

$$dE_{kp} = \frac{1}{2} \rho_p (A_{0p}\omega_p)^2 (L + 2h_p \tan\alpha)^2 e^{-2\frac{\psi_p h_p}{h_p}} dh_p \qquad\qquad 31$$

$$dE_{kp} = \frac{1}{2} \rho_p (A_{0p}\omega_{0p})^2 (L^2 + 4h_p L \tan\alpha + 4h_p^2 \tan^2\alpha) e^{-2\frac{\psi_p h_p}{\lambda_p}} dh_p \qquad\qquad 32$$

If we now integrate equation 32 to find the total kinetic energy of the vibrating column, we would also be able to find the total volume that has been energised. So

$$E_{kp} = \frac{1}{2} \rho_p (A_{0p}\omega_{0p})^2 \int_0^{h_p} (L^2 + 4h_p L \tan\alpha + 4h_p{}^2 \tan^2\alpha) e^{-2\frac{\psi_p h_p}{\lambda_p}} dh_p \qquad\qquad 33$$

In order to solve this integral, it should be divided into three separate equations:

$$E_{kp1} = \frac{1}{2} \rho_p (A_{0p}\omega_{0p})^2 \int_0^{h_p} (L^2) e^{-2\frac{\psi_p h_p}{\lambda_p}} dh_p \qquad\qquad 34a$$

$$E_{kp2} = \frac{1}{2}\rho_p (A_0\omega_{0p})^2 \int_0^{h_p} (4L\tan\alpha)h_p e^{-2\frac{\psi_p h_p}{\lambda_p}}\,dh_p \qquad\qquad 34b$$

$$E_{kp3} = \frac{1}{2}\rho_p (A_{0p}\omega_{0p})^2 \int_0^{h_p} (4\tan^2\alpha)h_p^2 e^{-2\frac{\psi_p h_p}{\lambda_p}}\,dh_p \qquad\qquad 34c$$

The solution of equation 34a is

$$E_{kp1} = \frac{1}{2}\rho_p (A_{0p}\omega_{0p})^2 e^{-2\frac{\psi_p h_p}{\lambda_p}}\left[-L^2\frac{\lambda_p}{2\psi_p}\right] \qquad\qquad 35$$

The part in brackets of the equation represents the volume. Since volume can't be negative, we must use the absolute value and the volume contribution of the first part of the integral is:

$$V_{1p} = L^2\frac{\lambda_p}{2\psi_p} \qquad\qquad 36$$

The solution of equation 34b is:

$$E_{kp2} = \frac{1}{2}\rho_p (A_{0p}\omega_{0p})^2 e^{-2\frac{\psi_p h_p}{\lambda_p}}\left[-2L\frac{h_p\lambda_p\psi_p}{\psi_p^2} - L\frac{\lambda_p^2}{\psi_p^2}\right]\tan\alpha \qquad\qquad 37$$

The volume in brackets if we substitute $h_p=\lambda_p/2\psi_p$ reduces to:

$$V_{2p} = 2L\left(\frac{\lambda_p}{\psi_p}\right)^2\tan\alpha \qquad\qquad 38$$

The solution of equation 34c is:

$$E_{kp3} = \frac{1}{2}\rho_p(A_{0p}\omega_{0p})^2 e^{-2\frac{\psi_p h_p}{\lambda_p}}\left[-\frac{h_p^2\lambda_p}{2\psi_p^2} - \frac{\lambda_p^2 h_p}{2\psi_p^2} - \frac{\lambda_p^3}{4\psi_p^3}\right]4\tan^2\alpha \qquad 39$$

The volume in brackets if we substitute $h_p = \lambda_p/2\psi_p$ reduces to:

$$V_{3p} = \frac{5}{2}\left(\frac{\lambda_p}{\psi_p}\right)^3 \tan^2\alpha \qquad 40$$

The total volume $V_{0p} = V_{1p} + V_{2p} + V_{3p}$. This implies that

$$V_{0p} = \frac{L^2\lambda_p}{2\psi_p} + 2L\left(\frac{\lambda_p}{\psi_p}\right)^2 \tan\alpha + \frac{5}{2}\left(\frac{\lambda_p}{\psi_p}\right)^3 \tan^2\alpha \qquad 41$$

2.2.3 Determination of the density

In order to obtain the density of the vibrating volume it is then logical that we should divide M_0 by equation 41:

$$\rho_{0p} = \frac{M_{0p}}{\frac{L^2\lambda_p}{2\psi_p} + 2L\left(\frac{\lambda_p}{\psi_p}\right)^2 \tan\alpha + \frac{5}{2}\left(\frac{\lambda_p}{\psi_p}\right)^3 \tan^2\alpha} \qquad 42$$

If the diffusion angle of the waves from the edges of the square edifice $\alpha\cong0$, as we expected, equation 42 reduces to:

$$\rho_{0p} = \frac{M_{0p}}{\left(\frac{L^2\lambda_p}{2\psi_p}\right)} \qquad 43$$

To obtain λ_p, we have to obtain the velocity of the medium. This can be achieved by doing a small seismic refraction survey, employing a geophone spacing of 0.5m. It is also

necessary to use the frequency f_p of the vibrating volume V_{0p}. This can be obtained form the linear plot in Figure 2.3. The angular frequency ω_b of the vibrating volume V_{0p} can be found where the line intercepts with the Y-axis.

The attenuation constant ψ_p can be estimated by calculating the damping factor Q_p from the seismic trace.

2.3 S-wave model

2.3.1 Determination of the mass M_{0s}.

In order to try and derive a mathematical model for the s-wave situation, we also assume a very simple mass on a spring model. Since the mass on the spring that oscillates in the s-wave (lateral) direction has host rock on both sides, it can be visualised in Figure 2.6.
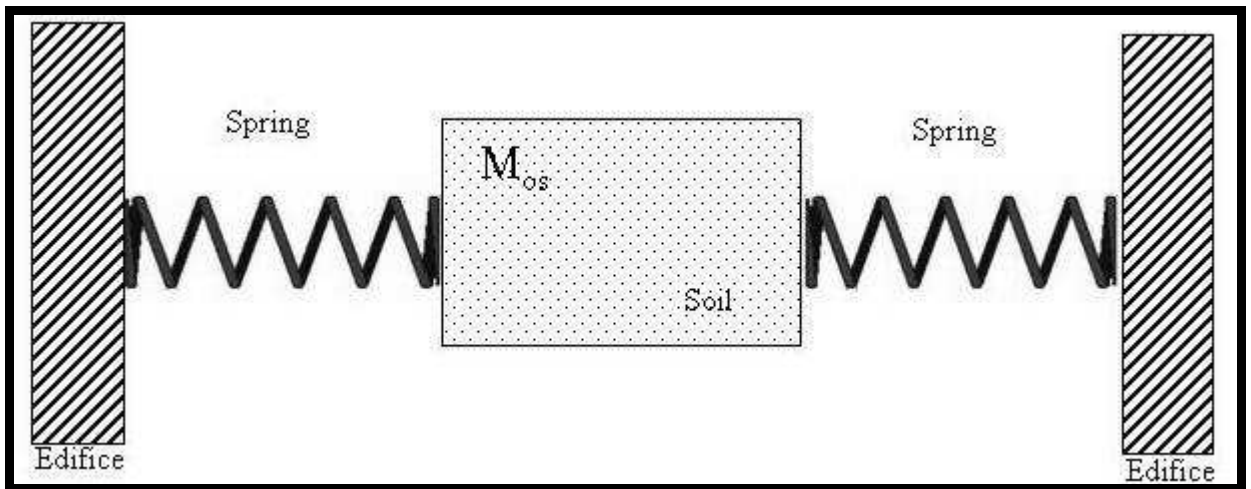
Figure 2.6: Schematic representation of the S-wave model as a mass between two springs.

If we make the assumption that the lateral dimension of the volume we sample is so small that the values of the spring constants are the same, we will be able to write:

$$F_s + k_s x_s = -k_s x_s \qquad\qquad 44$$

22

Thus from Newton II:

$$M_{0s}\ddot{x}_s + 2k_s x_s = 0 \qquad\qquad 45$$

$$\ddot{x}_s + \frac{2k_s}{M_{0s}} x_s = 0 \qquad\qquad 46$$

Thus

$$\omega_{0s}^2 = \frac{2k_s}{M_{0s}} \qquad\qquad 47$$

If we add a mass Δm to the mass M_{0s} and k_s stays the same, the angular frequency changes to ω_{1s}. Equation 47 can then be written as:

$$2k_s = \omega_{1s}^2 (M_{0s} + \Delta m) \qquad\qquad 48$$

And

$$\frac{1}{\omega_{1s}^2} = \frac{1}{2k_s}(M_{0s} + \Delta m) \qquad\qquad 49$$

Similarly to equation 9, equation 49 is a straight line with two unknowns, k_s and M_{0s}. We can thus transform equation 49 into:

$$\frac{1}{\omega_{1s}^2} = \frac{M_{0s}}{2k_s} + \frac{\Delta m}{2k_s} \qquad\qquad 50$$

Similarly, since $M_{0s}/2k_s$ is an unknown, it is also constant, say y_s.

$$\frac{1}{\omega_{1s}^2} = y_s + \frac{\Delta m}{2k_s} \qquad\qquad 51$$

$$\frac{1}{\omega_{1s}^2} = \frac{1}{2k_s}\Delta m + y_s \qquad\qquad 52$$

If we now plot Δm against $1/\omega_{1s}^2$, the slope of the line will be $1/k_s$. M_{0H} can be obtained from y or by the extension of the line. Where the line intersects with the Δm axis, the absolute value of M_{0s} can be read off. These values are accurate since the line is straight (Figure.2.7).
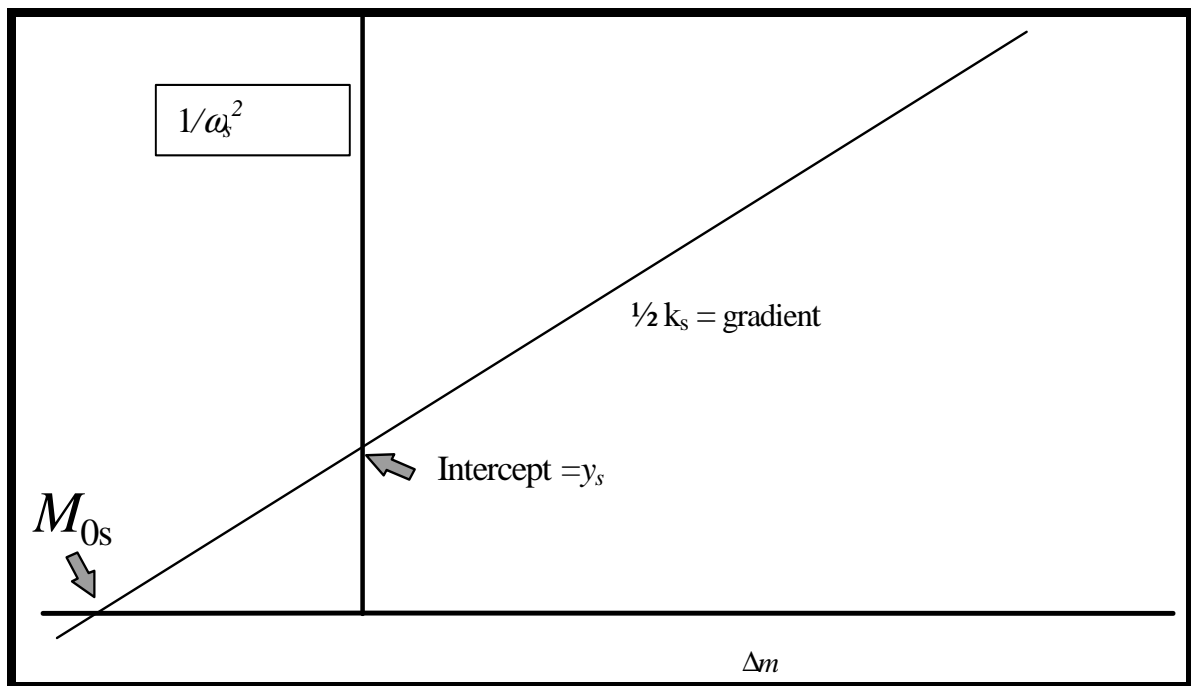

$1/\omega_s^2$

$\frac{1}{2}\,k_s = \text{gradient}$

Intercept $= y_s$

M_{0s}

Δm

Figure 2.7: Determination of the excited mass by the Shear wave.

2.3.2 Determination of the volume V_{0s}.

Similarly, if we assume that we are going to use a rectangular base plate with dimensions L, and if the diffusion angle from the plate is α, then the resulting area underneath the plate (Figure. 2.8) is the following:
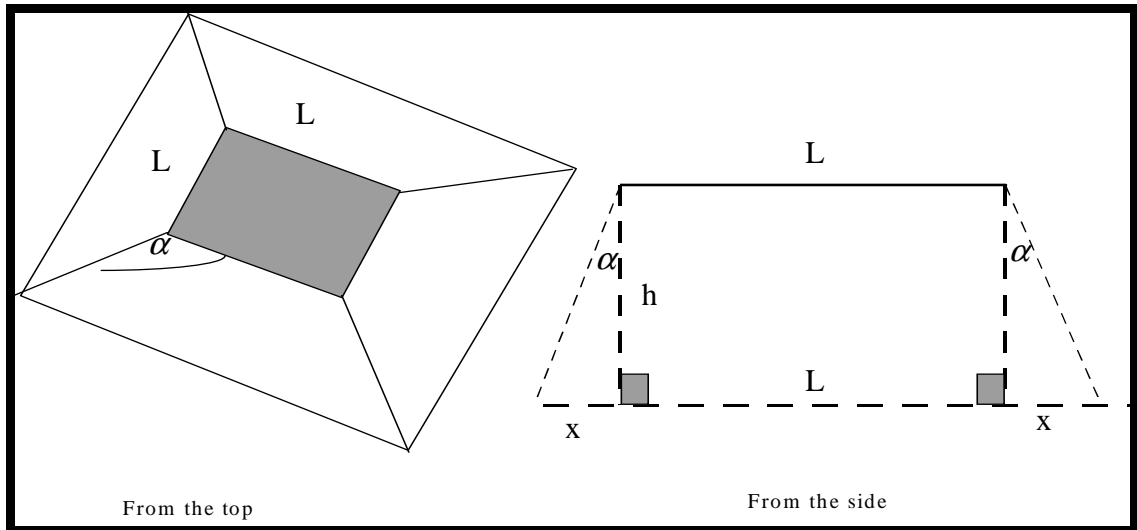
Figure 2.8: Area of influence under the base plate

The new length is L +2x and since tanα=x/h the new area is:

$$A = (L + 2h_s \tan \alpha)^2 \qquad\qquad 53$$

The volume of the vibrating column $V_{0s} = A \times h_s$. The height of the vibrating volume is unknown. The objective is to express the height of the volume in terms of elements that we can measure, like the wavelength or the velocity of seismic waves.

During the excitation of the ground mass, the movement experiences attenuation. The differential equation that expresses the system is at follows:

$$F_s + b_s V_s + k_s x_s = -k_s x_s \qquad\qquad 54$$

Where b_s is the attenuation coefficient and V_s is the velocity of the medium.

If we assume that the attenuation factor is dependant on the velocity of the ground movement and that x_s is the differential movement of a differential volume under the plate, then:

$$m_{0s} \frac{d^2 x_s}{dt^2} + b_s \frac{dx_s}{dt} + 2k_s = 0 \qquad\qquad 55$$

And if we substitute $2k_s = \kappa_s$

$$\frac{d^2 x_s}{dt^2} + \frac{b_s}{m_{0s}} \frac{dx_s}{dt} + \frac{\kappa_s}{m_{0s}} = 0 \qquad\qquad 56$$

And

$$\frac{d^2 x_s}{dt^2} + \frac{b_s}{m_{0s} \omega_{0s}} \omega_{0s} \frac{dx_s}{dt} + \omega_{0s}^{2} x_s = 0 \qquad\qquad 57$$

$$\frac{d^2 x_s}{dt^2} + 2\varepsilon_s \omega_{0s} \frac{dx_s}{dt} + \omega_{0s}^{2} x_s = 0 \qquad\qquad 58$$

where $\qquad \varepsilon_s = \dfrac{1}{2} \dfrac{b_s}{m_s \omega_{0s}}$.

As previously, the solution to this differential equation is:

$$A_s(\varepsilon) = A_0 e^{-\varepsilon \omega_{0H} t} \qquad\qquad 59$$

This is a harmonic oscillation that decays exponentially with time. We can express ε in terms of the quality factor Q_s:

$$\varepsilon_s = \frac{1}{2Q_s} \qquad\qquad 60$$

Thus equation 59 changes to:

$$A_s(\varepsilon) = A_{0s}e^{-\omega_{0s}t/2Q_s}$$ 61

Q is defined in terms of the fractional loss of energy per cycle of oscillation. In other words:

$$\frac{1}{Q_s} = \frac{-\Delta E_s}{2\pi E_s}$$ 62

The quality factor can also be expressed in terms of the logarithmic decrement:

$$Q_s = \frac{\pi}{\delta_s}$$ 63

If we now substitute equation 62 and the fact that t=x/v and ω=2πf into equation 61 we get:

$$A_s(\varepsilon) = A_{0s}e^{-(\frac{f_s\pi}{Q_sV_s})x_s}$$ 64

This transforms to

$$A_s(\varepsilon) = A_{0s}e^{-\frac{\psi_sx_s}{\lambda_s}}$$ 65

Where $f_s/V_s = 1/\lambda_s$ and $\pi/Q_s = \psi_s$. Equation 65 expresses the decrease in amplitude of a wave due to attenuation as a function of distance travelled. ψ_s is an attenuation constant that is frequency dependant. High frequency waves will attenuate more quickly. If we now want to express the decrease in amplitude as a function of depth h_s, we get

$$A_s(\varepsilon) = A_{0s}e^{-\frac{\psi_sh_s}{\lambda_s}}$$ 66

The depths that would be investigated will be quite small, and in the order of 3-10m. We can thus assume that the velocity at a depth h of the seismic wave is V_s . If we assume

27

that there is no frequency dispersion at these shallow depths ($\omega_{hs} = \omega_0$, and ω_0 is on the ground at h = 0), we can write:

$$V_s = A_{0s}\omega_{0s}e^{-\frac{\psi_s h_s}{\lambda_s}}$$

67

The kinetic energy of the column will be equal to the energy of the source. If we now attempt to calculate the kinetic energy of the vibrating column, we get:

$$E_{ks} = \frac{1}{2}m_s V_s^2$$

68

If we now look at the kinetic energy of a small volume at a depth h_s, and that $m_s = \rho_s * V_s$ and that Volume (V_s) = A * h_s we get

$$dE_{ks} = \frac{1}{2}\rho A V_s^2 dh_s$$

69

And if we substitute equations 13 and 29

$$dE_{ks} = \frac{1}{2}\rho_s(A_{0s}\omega_{0s})^2(L + 2h_s\tan\alpha)^2 e^{-2\frac{\psi_s h_s}{\lambda_s}} dh_s$$

70

$$dE_{ks} = \frac{1}{2}\rho_s(A_{0s}\omega_{0H})^2(L^2 + 4h_s L\tan\alpha + 4h_s^2\tan^2\alpha)e^{-\frac{2\psi_s h_s}{\lambda_s}} dh_s$$

71

If we now integrate equation 71 to find the total kinetic energy of the vibrating column, we would also be able to find the total volume that has been energised. So

$$E_{ks} = \frac{1}{2}\rho_s(A_{0s}\omega_{0s})^2\int_0^{h_s}(L^2 + 4h_s L\tan\alpha + 4h_s^2\tan^2\alpha)e^{-2\frac{\psi_s h_s}{\lambda_s}} dh_s$$

72

In order to solve this integral, it should be divided into three separate equations:

$$E_{ks1} = \frac{1}{2}\rho_s (A_{0s}\omega_{0s})^2 \int_0^{h_s} (L^2) e^{-2\frac{\psi_s h_s}{\lambda_s}} dh_s \qquad \text{73a}$$

$$E_{ks2} = \frac{1}{2}\rho_s (A_{0s}\omega_{0s})^2 \int_0^{h_s} (4L\tan\alpha) h_s e^{-2\frac{\psi_s h_s}{\lambda_s}} dh_s \qquad \text{73b}$$

$$E_{ks3} = \frac{1}{2}\rho_s (A_{0s}\omega_{0s})^2 \int_0^{h_s} (4\tan^2\alpha) h_s^2 e^{-2\frac{\psi_s h_s}{\lambda_s}} dh_s \qquad \text{73c}$$

The solutions of equation 73a, 73b and 73c are the same as for the Z-component.

The total volume $V_{0s} = V_{1s} + V_{2s} + V_{3s}$. This implies that:

$$V_{0s} = \frac{L^2 \lambda_s}{2\psi_s} + 2L\left(\frac{\lambda_s}{\psi_s}\right)^2 \tan\alpha + \frac{5}{2}\left(\frac{\lambda_s}{\psi_s}\right)^3 \tan^2\alpha \qquad \text{74}$$

2.3.3 Determination of the density

In order to obtain the density of the vibrating volume it is then logical that we should divide M_s by equation 74:

$$\rho_{0s} = \frac{M_{0s}}{\dfrac{L^2 \lambda_s}{2\psi_s} + 2L\left(\dfrac{\lambda_s}{\psi_s}\right)^2 \tan\alpha + \dfrac{5}{2}\left(\dfrac{\lambda_s}{\psi_s}\right)^3 \tan^2\alpha} \qquad \text{75}$$

If the diffusion angle of the waves from the edges of the square edifice $\alpha \cong 0$, as we expected, equation 75 reduces to:

29

$$\rho_{0s} = \frac{M_{0s}}{\left(\dfrac{L^2 \lambda_s}{2\psi_s}\right)}$$

76

To obtain λ_s, we have to obtain the velocity of the medium. This can be achieved by doing a small seismic refraction survey, employing a geophone spacing of 0.5m. It is also necessary to use the frequency f_s of the vibrating volume V_s. This can be obtained form the linear plot in Figure 2.6. The angular frequency ω_{0H} of the vibrating volume V_{0s} can be found where the line intercepts with the Y-axis.

The attenuation constant ψ_s can be estimated by calculating the damping factor Q_s from the seismic trace.

2.4 The multi layered situation

2.4.1 Introduction

In almost all of the cases, a single layer only scenario will not be encountered. Since this technique will almost always be used as an engineering application, the weathered layer will mostly be investigated. The weathered layer is in exceptional cases only single layer. It is usually at least two layers and then the bedrock. At the surface, it usually consists of a lower density soil cover, and then of higher density clays or semi weathered soils (Figure 2.9).

2.4.2 Multilayer mathematical approach

During a density sounding the aim is to obtain the densities of the individual layers. The objective is also the same with other geophysical methods, like the D.C. Resistivity method. The total resistivity at the surface is obtained by summing the individual layer resistivities which are in series (Telford et al., 1986).
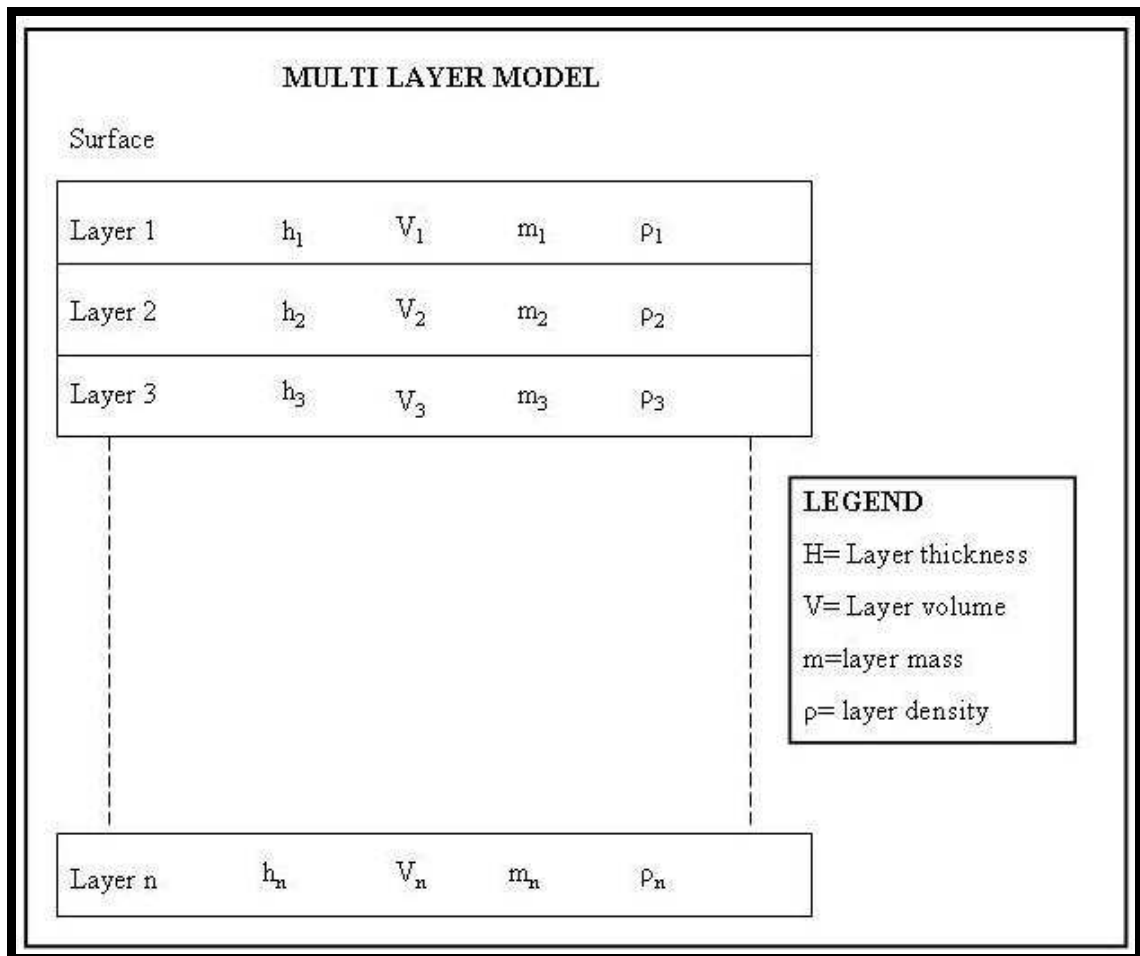
$$R_t = \sum_{n=1}^{n} R_n = R_1 + R_2 + R_3 + \ldots\ldots\ldots + R_n \qquad\qquad 77$$

MULTI LAYER MODEL

Surface				
Layer 1	h_1	V_1	m_1	ρ_1
Layer 2	h_2	V_2	m_2	ρ_2
Layer 3	h_3	V_3	m_3	ρ_3

LEGEND

H= Layer thickness

V= Layer volume

m=layer mass

ρ= layer density

Layer n	h_n	V_n	m_n	ρ_n

Figure 2.9: Schematic diagram of the layering in a weathered layer.

Unfortunately, the densities of the different layers cannot be added together to get a total density, but the masses and the volumes of the different layers can be added. So,

$$\rho_t \neq \sum_{n=1}^{n} \rho_n \neq \rho_1 + \rho_2 + \rho_3 + \ldots\ldots\ldots + \rho_n \qquad\qquad 78$$

but

$$m_t = \sum_{n=1}^{n} m_n = m_1 + m_2 + m_3 + \ldots\ldots + m_n \qquad\qquad 79$$

and

$$V_t = \sum_{n=1}^{n} V_n = V_1 + V_2 + V_3 + \ldots\ldots\ldots\ldots + V_n \qquad\qquad 80$$

This translates back to layer thicknesses:

$$h_t = \sum_{n=1}^{n} h_n = h_1 + h_2 + h_3 + \ldots\ldots\ldots\ldots + h_n \qquad\qquad 81$$

By obtaining different masses and different volumes separately, it is possible to obtain the densities for the different layering.

2.4.3 Depth of penetration and layer thickness

It has been shown that the penetration into and the return of high frequencies from the earth is affected and limited by attenuation and energy losses due to reverberation and transmission losses. Changes in frequency content also occurs (Waters, 1981). To a first approximation the loss of amplitude follows an exponential law:

$$A(z) = A_0 e^{-\alpha z} \qquad\qquad 82$$

where α is the attenuation constant.

By following the same reasoning as in equations 14 to 28 and 54 to 67, the attenuation constant α can be written as:

$$\alpha = \frac{\pi \times f}{Q \times V} \qquad\qquad 83$$

Where f is the frequency, V is the velocity and Q is the quality factor.

The 1/Q factor that is embedded into equation 83 is called the Specific dissipation constant (Griffiths and King, (1969), Waters, (1981), Kibble, (1985) and Sears et. al,

(1987)). It is a measure of how vibrational energy is dissipated.

It is thus true that α depends on the following factors:

- It is frequency dependant. Higher frequency results in higher attenuation.
- High velocity, and thus high density, results in a slower attenuation

This means that for layers in the weathered layer, the following scenarios may occur:

- If the velocity and the density of the layer are low, higher frequencies will be attenuated quickly and will be removed from the signal.
- If the velocity and the density of the layer are higher, the higher frequencies will be preserved.
- The lower density layers are usually near the surface. It thus filter out the higher frequencies (earth is acting as a low pass filter), and lower frequencies are associated with deeper layering.

CHAPTER 3

Development of dedicated software

3.1 Introduction

After the theoretical development of the method was completed, data had to be collected in the field to test and evaluate the theory. Dedicated software to process the density sounding data did not exist. The approach was to first test the method on a homogeneous single layer situation of mafic rocks. This was mainly to test the validity of the method, but also because it would be easier to process the single layer data by using different software.

The data of the first two soundings at Leeuwfontein (Figure 4.5) was processed by using Seisan™. This commercial software package is developed to process earthquake seismic data. Seisan™ can calculate a Power-frequency spectrum of the trace, which forms the heart of the density sounding data processing. The data obtained from these single layer soundings proved to be encouraging and a single layer only situation was surveyed on a weathering profile.

Previous knowledge of the geology at Donkerhoek (Figure 4.11) was the main decision for the second field test.   A detailed geophysical study was done at Donkerhoek to obtain the best position for the Core Library buildings (Craill et al, 1993). It showed the areas where the weathering profile was more than 3m thick. This is theoretically thick enough to represent a single layer case.

Changes were also made to the equipment for easier handling. This forced the development of test software in Matlab™ and Scilab. The software developed in Matlab™ proved to be a little easier to use than Sisan™. The processing of the data was limited to computers that have a copy of Matlab™. Dedicated software had to be developed for this method, using programming software capable of producing executables.

3.2 Development of dedicated software to process the density sounding data

The software to process this data was developed in Visual Basic because it was:

- Easy to develop, as basic is a fairly easy programming language
- Easy to make changes
- Cheap, as the visual basic package is not that expensive
- Possible to create files that would install and run on any computer with windows, even if visual basic is not installed.
- Created Data files are in files that are compatible with Excel, which makes it easy to access.
- The determination of the frequency is the most important aspect, while processing this data. The most important calculation that this program must perform, is to determine the power spectrum of the seismic trace. The determination of the excited mass, the small movement elasticity modulus and the depth of investigation depend on the accurate determination of the frequency. Various methods were develop to make the Graphical User Interface (GUI) around this more user friendly.

3.2.1 Using the software

The developed processing software is called Seisrho. The "New Project" tag is selected when the processing of a new sounding is started. The "Open project" tag is selected when one works on a previously created or existing project. If the "New Project" tag is selected it activates the rest of the tags. A directory called "rawdata" and a directory called "segydata" are created during this process.

Sounding data is gathered using a seismograph. At this stage two seismographs are supported: - the 24 - channel Bison 8026 and the 24 - channel Geometrics Strataview. The data is transferred from the seismographs to the computer using

Mirror – III in the case if the Bison seismograph and Laplink for the Geometrics seismograph. The process is quite simple. Download or Laplink the raw seismograph data of the density sounding into the created directory called "rawdata".

The data in the specific seismograph format is then imported into the Seisrho package using the "Import Data" tag under the "File" menu (Figure 3.1). A single file can be imported, while the option for all data files to be imported also exists. (Figure 3.2). The program default is to look for the seismograph data in the directory "rawdata". The data is then imported and in the process it is converted into SEGY format, which is the industry standard for seismic related data. During the import and conversion of the data, the data is stored in the created directory called "segydata".
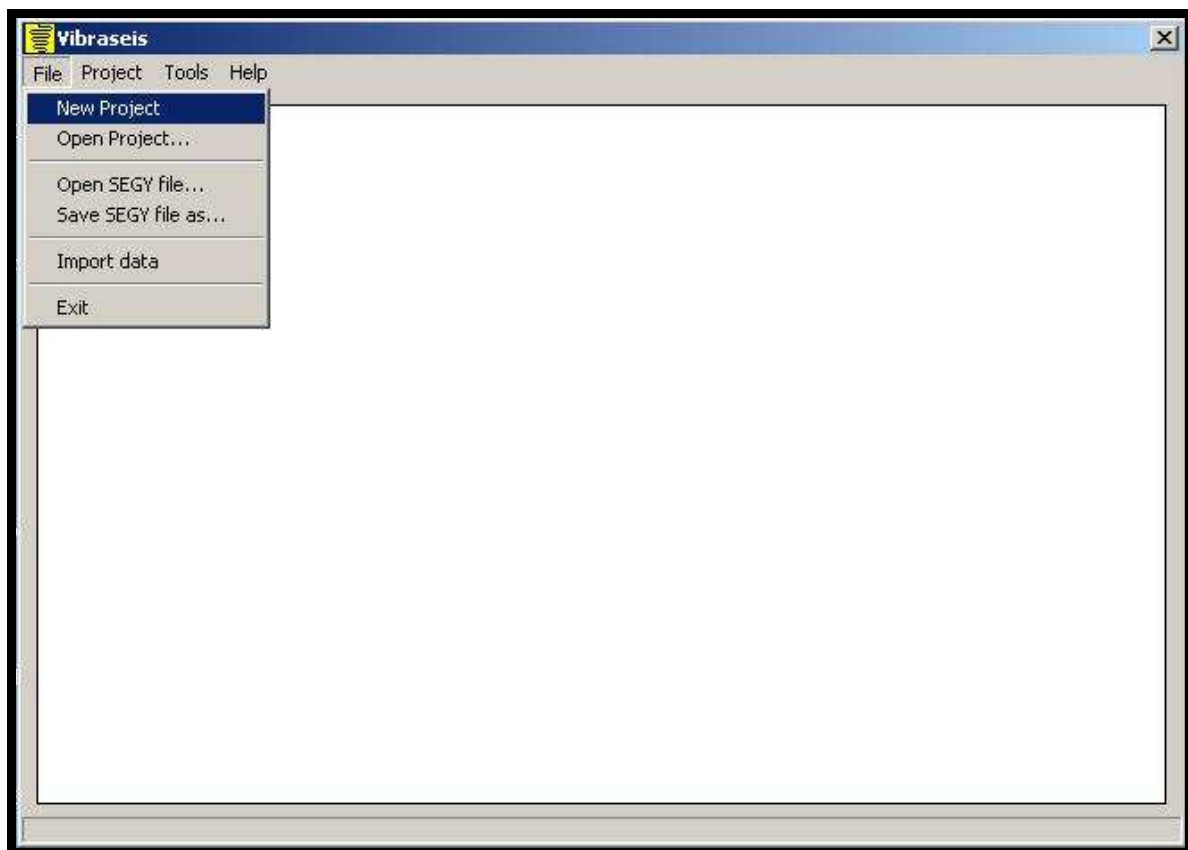
Figure 3.1:   The main menu when the software package Seisrho is executed.
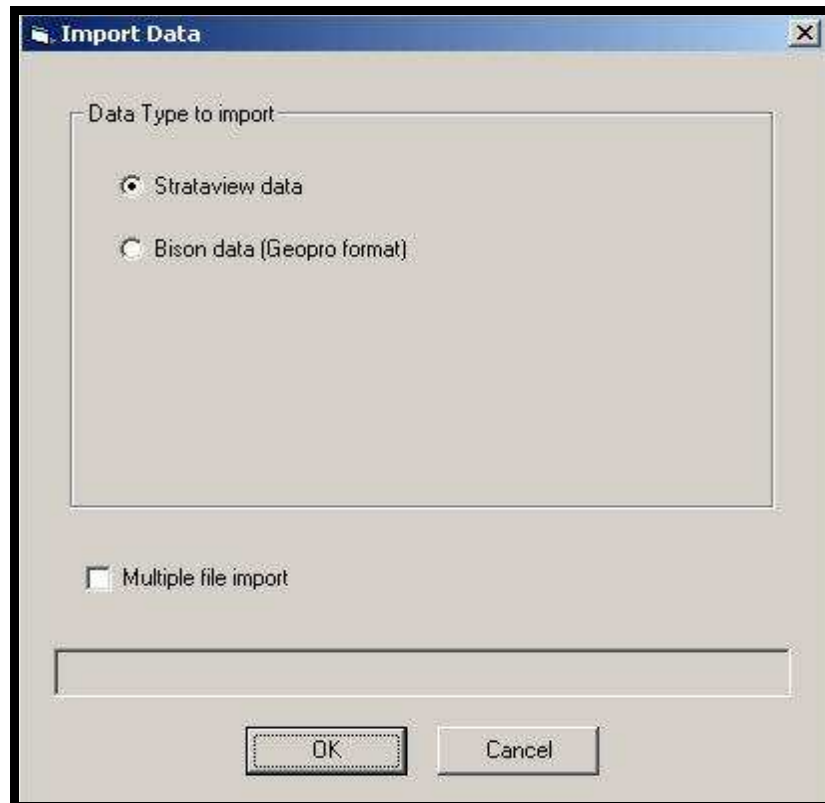
Figure 3.2:   Data import screen of the Seisrho package

The data in the "segydata" directory is the data to be used for further for the processing.   Inside this directory, subdirectories called "layer1" up to "layer n" (depending on the chosen number of layers) will be created.   All the relevant processing information for each layer will be stored inside the specific directory. This will also include files that contain all the filtering and Q-factor information, which is used to calculate the density of each layer.

The first step during the processing of the density sounding is to obtain the excited ground masses of the different layers present. This option can be selected from the main menu as "Pick Frequencies and Calculate Mass (Figure 3.3).   This is done for all three components, X, Y and Z.   The method on how the excited ground masses are calculated is explained in Fourie and Cole (CGS report 2004-0095) and involves a plot of $1/\omega^2$ vs added mass to obtain a straight line. The excited ground mass is the position where this line intersects the Y-axis.
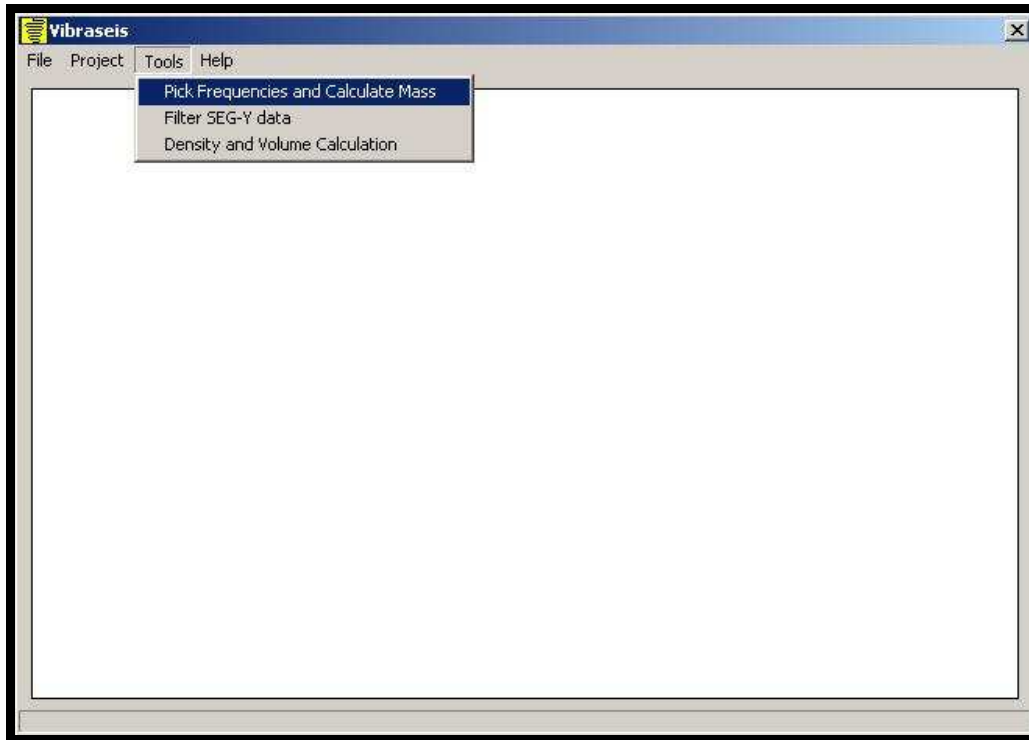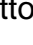
Figure 3.3:   Pick frequencies and calculate mass on the main menu

All three components can be chosen for analysis by selecting the "X", "Y" or "Z" option.   The excited ground mass of more than one layer can be determined by using this interface.   Figure 3.4 shows the main interface for mass calculation.   An extra layer is added by clicking on the F button.   A layer can be removed if the ✗F button is selected.   The display of the power spectrum in the top window can be customised by selecting the frequency window under the "Power Spectrum" option. Dominant frequencies are then selected by the ► or ◄ buttons and by moving the cursor towards the main peaks and press the mouse button to select the frequency. The next and previous shot records can be selected by pressing the ➡ or ⬅ buttons.

This chosen frequency is then used to automatically calculate a mass.   The bottom window displays the line that is fitted through the data.   A direct estimation of the mass and k-value is given on a continuous basis.
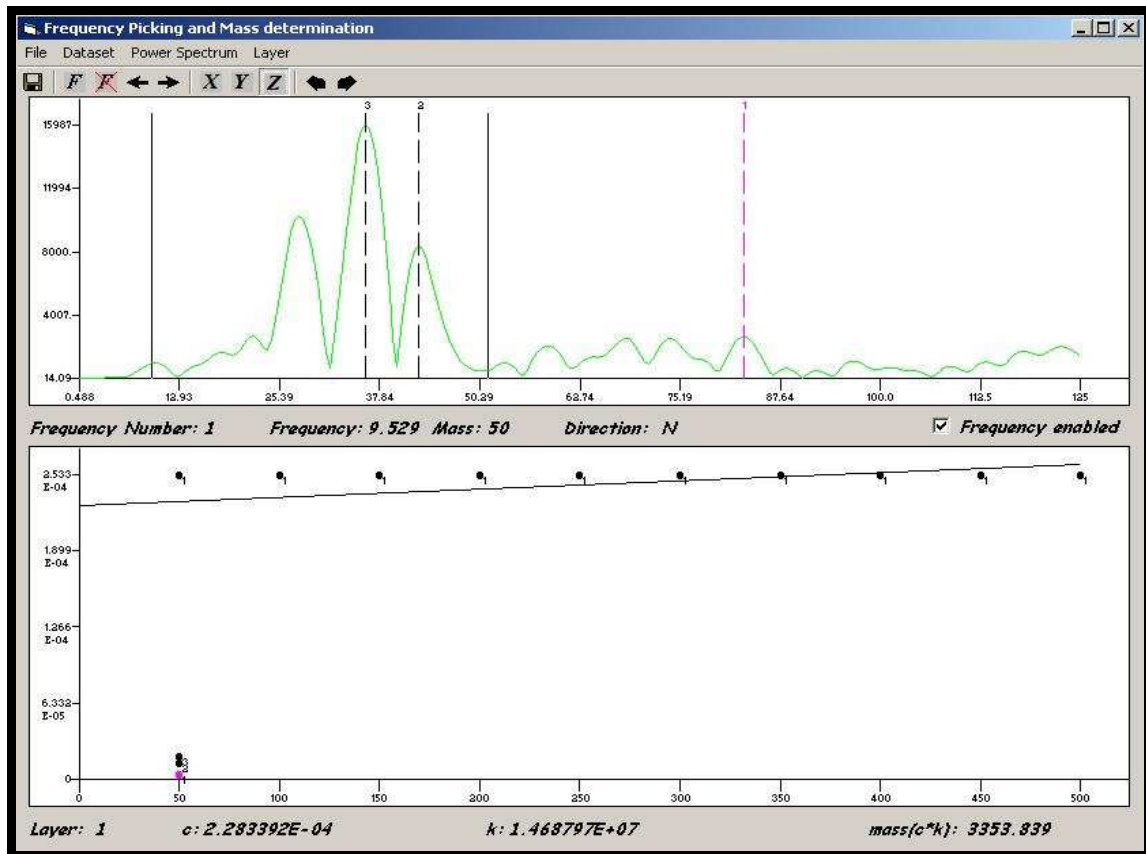
Figure 3.4: Main mass calculation interface.

The next step in the processing is to identify the different frequencies that are associated with the different layers of the weathered zone. Each original trace is then filtered more than once to obtain these dominant frequencies, i.e. if there are three dominant frequencies, three different layers exist. The filtering will then be performed three times to produce three different traces correlating with these frequencies. These traces will be stored inside the "layer1" to "layer 3" directories hosted in the segydata directory. This option can be chosen from the main menu as the "Filter SEG-Y data" option (Figure 3.5).

Figure 3.6 shows the main interface where the filter parameters are chosen for the filter process. The parameters of the traces of all three components can be chosen and filtered by using this window. The next and previous records can be selected by pressing the ► or ◄ buttons.
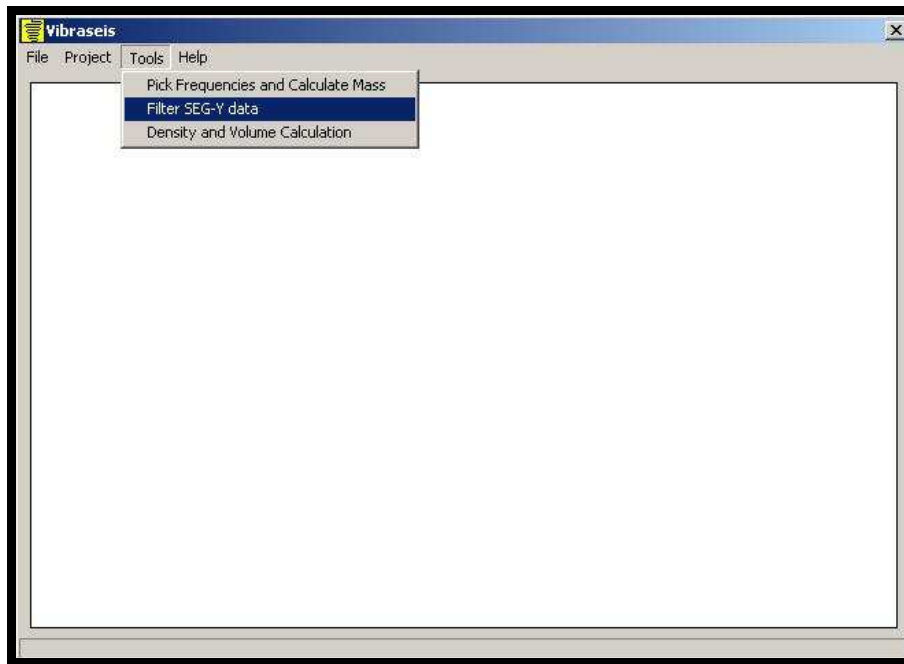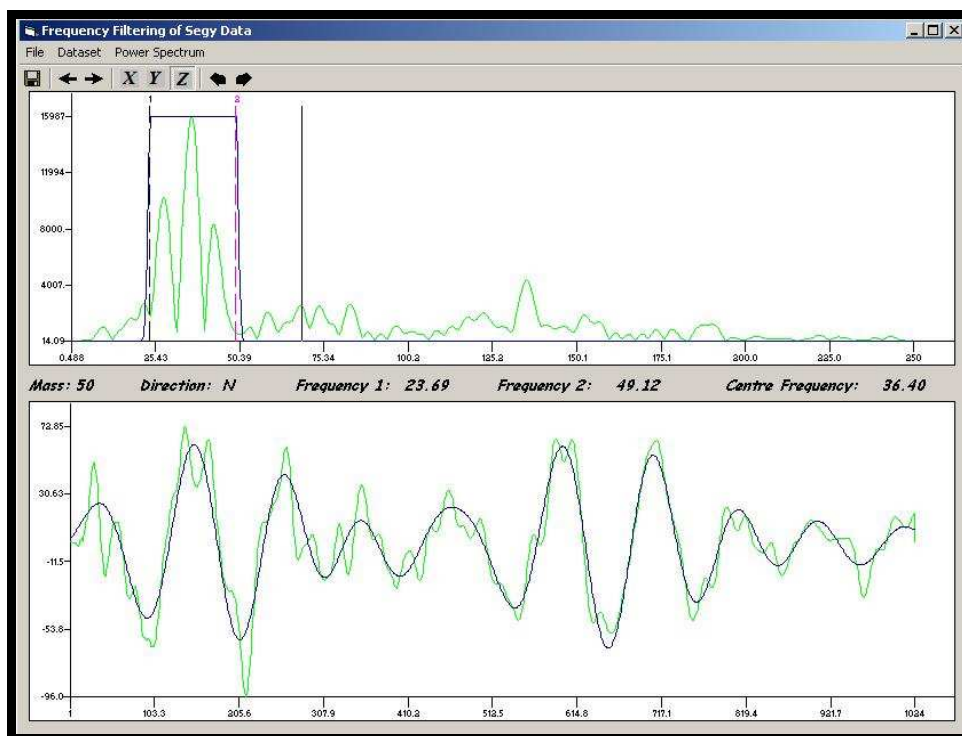
Figure 3.5:   Main menu to filter the segy data.

Figure 3.6:   Window to filter the segy trace data.   The lower and higher frequencies can be selected by pressing the ← or → buttons.   The frequencies between the lines are kept.
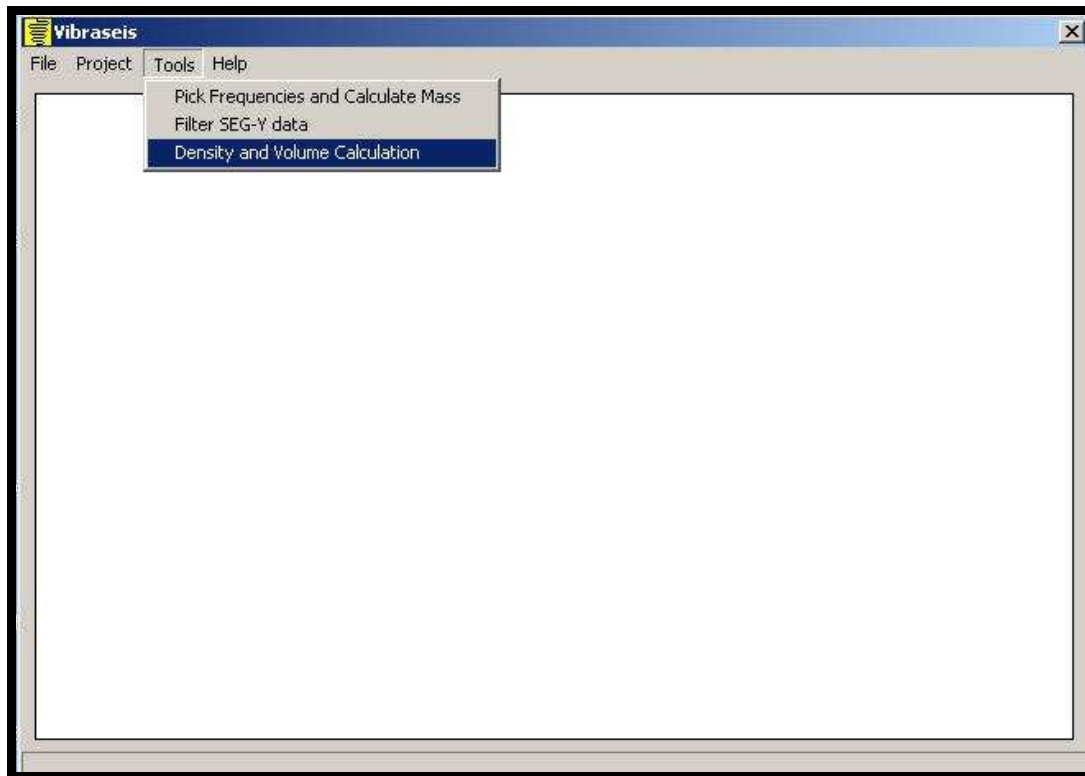
Figure 3.7:   Main menu of Density and Volume Calculation.

The last step in the processing sequence is to calculate the volume of the excited mass and then obviously the density.   This option can be selected from the main menu (Figure 3.7).   The window, in which the main volume and density calculations are performed, is shown in Figure 3.8.   This process has to be repeated for each frequency and each trace.   Each component is done within its own window.

The top window displays the power spectrum of the filtered trace, as a guide.   The middle window displays the filtered trace while the bottom window shows the values of the Q-factor.   These Q-factors are calculated on a cycle to cycle basis and it is possible to remove a cycle from the equation if it does not fit in with the data, due to noise.   This is done to improve the accuracy and speed of the calculation. The next and previous records can be selected by pressing the ► or ◄ buttons.   The k-value (small movement elasticity modulus), the thickness of the layer and also the density of the layer are displayed at the bottom of this window. If the save button is pressed all the data is saved to a CSV file.   These files can easily be opened by

Excel. Finally the main menu (Figure 3.9) is used to create a summary file of all the parameters, in a CSV format. These are the final interpretation values of the density sounding.
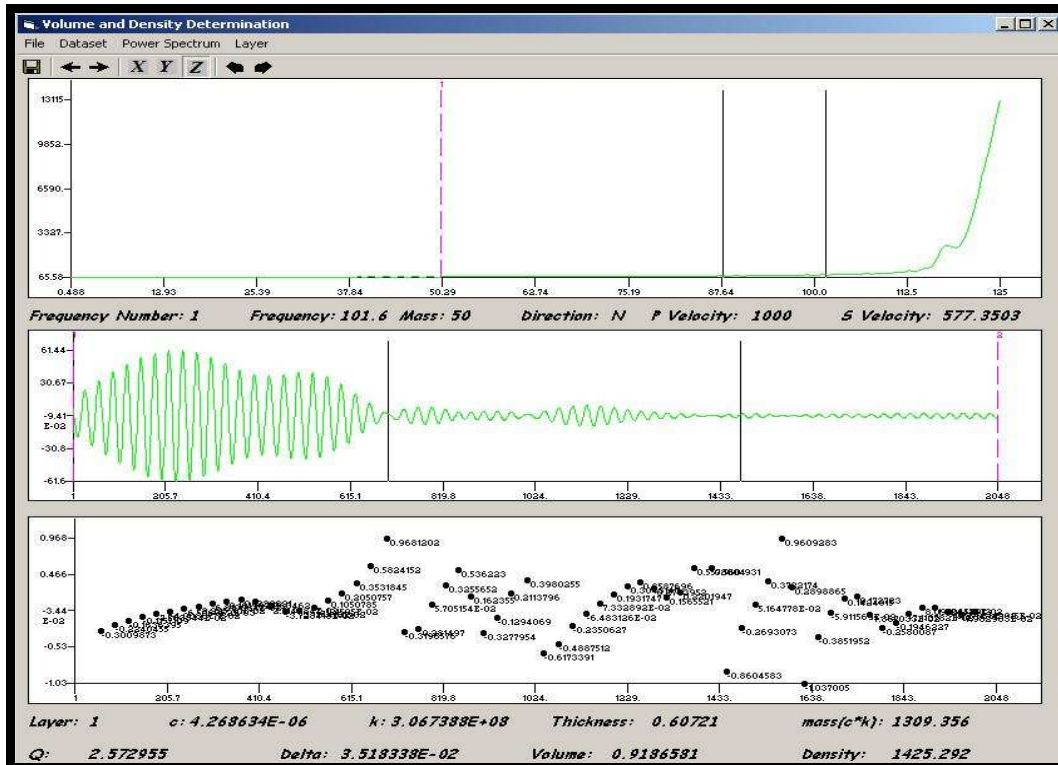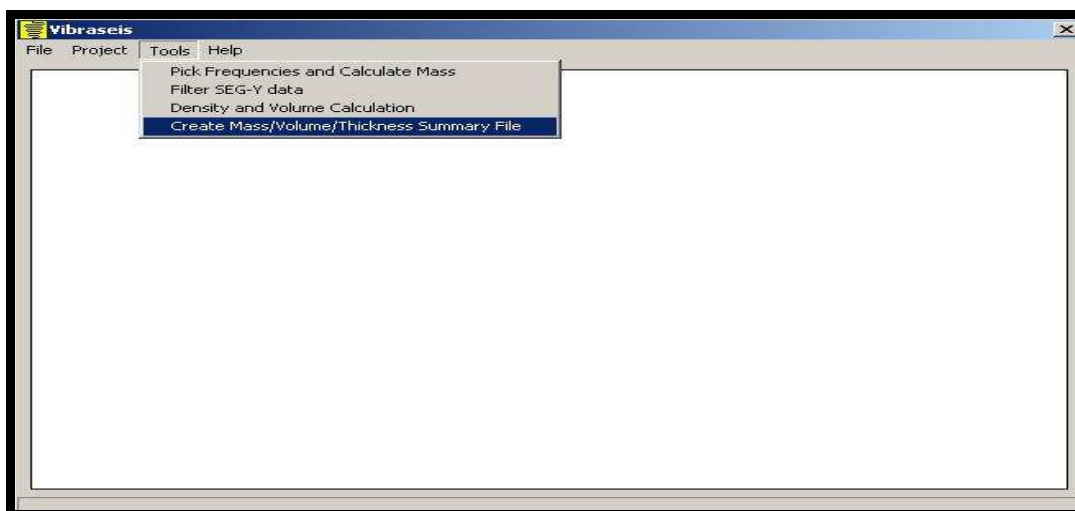

Figure 3.8: Main window to obtain volume and density.

Figure 3.9: Main menu to create summary interpretation file.